The Astrophysical Journal, 810:111 (10pp), 2015 September 10 doi:10.1088/0004-637X/810/2/111

CYANOMETHANIMINE ISOMERS IN COLD INTERSTELLAR CLOUDS: INSIGHTS FROM ELECTRONIC STRUCTURE AND KINETIC CALCULATIONS

Fanny Vazart[1], Camille Latouche[1], Dimitrios Skouteris[1], Nadia Balucani[2], and Vincenzo Barone[1]
[1] Scuola Normale Superiore, Piazza dei Cavalieri 7, I-56125 Pisa, Italy
[2] Dipartimento di Chimica, Biologia e Biotecnologie, Universitá degli Studi di Perugia, Via Elce di Sotto 8, I-06123 Perugia, Italy
Received 2015 April 2; accepted 2015 May 31; published 2015 September 4

ABSTRACT

New insights into the formation of interstellar cyanomethanimine, a species of great relevance in prebiotic chemistry, are provided by electronic structure and kinetic calculations for the reaction $CN + CH_2 = NH$. This reaction is a facile formation route of *Z*,*E*-C-cyanomethanimine, even under the extreme conditions of density and temperature typical of cold interstellar clouds. *E*-C-cyanomethanimine has been recently identified in Sgr B2(N) in the Green Bank Telescope (GBT) PRIMOS survey by P. Zaleski et al. and no efficient formation routes have been envisaged so far. The rate coefficient expression for the reaction channel leading to the observed isomer *E*-C-cyanomethanimine is $3.15 \times 10\text{-}10 \times (T/300)^{0.152} \times e^{(-0.0948/T)}$. According to the present study, the more stable *Z*-C-cyanomethanimine isomer is formed with a slightly larger yield $(4.59 \times 10^{-10} \times (T/300)^{0.153} \times e^{(-0.0871/T)}$. As the detection of *E*-isomer is favored due to its larger dipole moment, the missing detection of the *Z*-isomer can be due to the sensitivity limit of the GBT PRIMOS survey and the detection of the *Z*-isomer should be attempted with more sensitive instrumentation. The $CN + CH_2 = NH$ reaction can also play a role in the chemistry of the upper atmosphere of Titan where the cyanomethanimine products can contribute to the buildup of the observed nitrogen-rich organic aerosols that cover the moon.

Key words: astrochemistry – ISM: molecules – methods: numerical – molecular processes

1. INTRODUCTION

The recent detection of *E*-cyanomethanimine in Sgr B2(N) in the Green Bank Telescope (GBT) PRIMOS survey by Zaleski et al. (2013) has raised the question of how this species is formed under the conditions of the cold interstellar medium (ISM). At the moment, the principal astrochemical databases for molecular formation routes in the ISM (UMIST12 and KIDA; Wakelam et al. 2012; McElroy et al. 2013) do not include any pathway for this species or its isomers. This situation can be improved by quantum mechanical (QM) calculations of spectroscopic and thermodynamic properties to guide and support observations, line assignments, and data analysis (Puzzarini et al. 2014a, 2014b). The possible formation of cyanomethanimine in the ISM starting from the widespread HCN and HNC species was amply scrutinized in the past because it was suggested by Chakrabarti & Chakrabarti (2000) that the oligomerization of HCN in the gas phase could lead up to adenine in four steps. Adenine is one of the purine RNA nucleobases and, having the gross formula $C_5H_5N_5$, can be viewed as a HCN pentamer. In the same fashion, cyanomethanimine is the dimer of HCN (or HNC, which is also ubiquitous in the ISM). The suggestion by Chakrabarti & Chakrabarti (2000) was disproved by Smith et al. (2001) who demonstrated that the first step of their sequence (that is, the formation of cyanomethanimine starting from two HCN molecules) is already impossible in the low-temperature interstellar environment. Later on, Yim & Choe (2012) and Jung & Choe (2013) also explored the possibility that the reaction between HCN or HNC with the protonated species $HCNH^+$ could lead to cyanomethanimine. Even though the presence of a proton substantially lowers the reaction barriers, Yim & Choe (2012) concluded that those reactions are not viable gas-phase routes to cyanomethanimmine formation in the ISM.

Because of the lack of gas-phase routes, after the detection of *E*-cyanomethanimine toward Sgr B2(N), Zaleski et al. (2013, p.5) suggested that "a radical chemistry formation route...could occur in interstellar ices." In this contribution, we demonstrate, instead, that the reaction between two widely diffuse species, that is, the cyano radical and methanimine, can easily account for cyanomethanimine formation under the characteristic conditions of interstellar clouds. The interaction of the $^{\cdot}CN$ radical with methanimine was already explored by Basiuk & Bogillo (2002). Their B3LYP/6-31++G(d,p) calculations demonstrated that the addition of the $^{\cdot}CN$ radical to the π bond of methanimine is barrierless but the reaction exit channels were not explored in that study. Nevertheless, in the low-density conditions of the ISM where no ternary molecular encounters take place, the stabilization of bound reaction intermediates could only take place via radiative emission, a process with very low probability, which is not competitive with bond fission when exothermic fragmentation channels are available.

Therefore, we have undertaken a detailed QM investigation relying on some work already performed on the thermodynamic, kinetic, and spectroscopic features of cyanomethanimine derivatives (*E*-C- and *Z*-C-; Vazart et al. 2015). We investigated the vibrational and thermochemical signatures of all stable molecules herein presented and the transition states connecting them (Figure 1), using one of the most reliable computational models rooted in the density functional theory (DFT) coupled to single point energy refinement by a coupled cluster (CC) approach in conjunction with complete basis set extrapolation (CBS-QB3). Computed reaction rate coefficients are also provided using a capture model and the Rice–Ramsperger–Kassel–Marcus (RRKM) method for the open reaction channels, which are

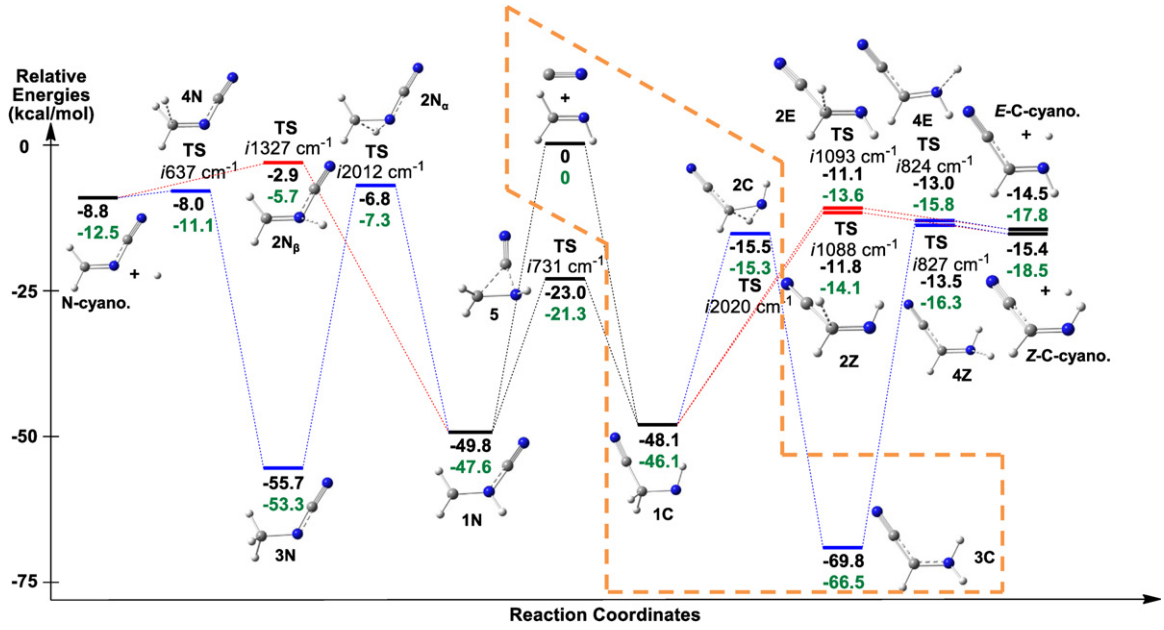

Figure 1. Full reaction paths of the reaction ˙CN + CH_2NH → *E*-C-, *Z*-C-, and N-cyanomethanimine with relative electronic energies (black) and zero-point corrected energy (green). The energies were computed using the CBS-QB3 level of theory. Alternative pathways in blue and red. The compounds investigated by Basiuk & Bogillo (2002) are in orange (dashed line).

$$CN + CH_2{=}NH$$

$$\rightarrow Z{-}NC{-}CH{=}NH + H \quad \Delta H_0^\circ = -18.5 \text{ kcal/mol} \quad (1)$$

$$\rightarrow E{-}NC{-}CH{=}NH + H \quad \Delta H_0^\circ = -17.8 \text{ kcal/mol} \quad (2)$$

$$\rightarrow CH_2{=}N{-}CN + H \quad \Delta H_0^\circ = -12.5 \text{ kcal/mol} \quad (3)$$

$$\rightarrow Z{-}CN{-}CH{=}NH + H \quad \Delta H_0^\circ = -2.2 \text{ kcal/mol} \quad (4)$$

$$\rightarrow E{-}CN{-}CH{=}NH + H \quad \Delta H_0^\circ = -1.5 \text{ kcal/mol} \quad (5)$$

(the indicated enthalpies of reactions are those calculated in this work; see below). As we are going to see, all *E*-C-, *Z*-C-, and N-isomers can be formed to some extent, but only *E*-C-cyanomethanimine has been identified so far in interstellar space. This fact needs to be critically discussed considering that the way used to characterize the compound was only through microwave spectroscopy. Indeed, as this technique strongly depends on the dipole moment of the molecule, the detection of the *E*-C- isomer is favored by a factor of 6 (cf. Zaleski et al. 2013). Therefore, the presence of *Z*-C- or N- isomers cannot be ruled out, given the sensitivity limits of the GBT PRIMOS survey.

2. COMPUTATIONAL DETAILS

All calculations have been carried out with a locally modified version of the Gaussian suite of programs (Frisch et al. 2014). Most of the computations were performed with the double-hybrid B2PLYP functional (Grimme 2006) in conjunction with the m-aug-cc-pVTZ basis set (Dunning 1989; Papajak et al. 2009), where the *d* functions on hydrogens have been removed. Semi-empirical dispersion contributions were also included in DFT computations by means of the D3 model of Grimme, leading to the B2PLYP-D3 functional (Grimme et al. 2010; Goerigk & Grimme 2011). The harmonic vibrational frequencies for minima and transition states have been obtained by diagonalizing the corresponding analytical Hessians (Biczysko et al. 2010). The energies reported in the following (except where noted) were computed using the Complete Basis Set (CBS-QB3) method, which leads to very accurate values by employing a CC ansatz in conjunction with complete basis set extrapolation (Ochterski et al. 1996; Montgomery et al. 2000).

On these grounds, rate constants have been obtained by a combination of capture theory and RRKM calculations using the same code we developed and described in previous papers (Leonori et al. 2009, 2013; Balucani et al. 2015b). The initial bimolecular rate constant of CN + CH_2NH is calculated using capture theory. Here, the assumption is that if the system has enough energy to surmount the centrifugal barrier, then it goes on to form one of the initial adducts. For a long range potential of the form $-\frac{C_6}{R^6}$, the capture cross section is given by the formula

$$\sigma(E) = \pi * 3 * 2^{-\frac{2}{3}} * \left(\frac{C_6}{E}\right)^{1/3}$$

where E is the translational energy. The corresponding rate constant is given by the cross section multiplied by the collision velocity $(2E/m)^{1/2}$, where m is the reduced mass of the reactants. It must be stressed that it is the translational (collision) rather than the total energy that appears in the capture rate expression. In order to account for the possibility that the reactants occupy higher internal states (and, consequently, have a lower collision energy), we performed a convolution of the raw capture rate constants with the probability density function for the internal energy (obtained from a simple calculation of the reactant internal density of states).

As the initial state of the reactants is assumed to be uncorrelated to the initial intermediate formed, the initial populations of the three possible intermediates are simply taken

to be proportional to their respective densities of states at the total energy considered. Moreover, the capture model furnishes us with the maximum value of J, the total angular momentum quantum number, as a function of total energy, which is subsequently used in the unimolecular calculations.

In order to calculate the rate of back-dissociation into reactants, we have used the principle of detailed balance which, for a reaction of the form A + B $\leftrightarrow$ C, would read

$$k(\mathrm{A}+\mathrm{B}\rightarrow \mathrm{C})*\rho(\mathrm{A}+\mathrm{B})=k(\mathrm{C}\rightarrow \mathrm{A}+\mathrm{B})*\rho(\mathrm{C})$$

where ρ(C) and ρ(A+B) are, respectively, the density of states of intermediate C and the density of states per unit volume of the bimolecular system A+B (including the three-dimensional relative motion). Thus, we calculated the rate of back-dissociation into reactants by multiplying the bimolecular capture rate constant with the total density of states per unit volume of CN+CH_2NH and dividing by the total density of states of the initial adducts (assuming, for each energy, a maximum value for the total angular momentum J given by the capture calculations).

After the initial intermediate is formed, the assumption is made that the available energy is statistically distributed among the various degrees of freedom (subject to conservation of total angular momentum) and therefore the RRKM model is suitable for the calculation of unimolecular rate constants. Moreover, in the RRKM model, the existence of a well-defined transition state is postulated for each elementary reaction, i.e., a configuration of "no recrossing," which, once crossed by the reactants, invariably leads to the products. The existence, in all cases, of a well-defined maximum in energy renders this assumption reasonable. The microcanonical rate constant for each elementary step is calculated using the formula

$$k(E)=\frac{N(E)}{h\rho(E)},$$

where $N(E)$ denotes the sum of states in the transition state at energy E, $\rho(E)$ is the reactant density of states at energy E, and h is Planck's constant. $N(E)$ is obtained by integrating the relevant density of states up to energy E and the rigid rotor/harmonic oscillator model is assumed. Both densities of states (reactant and transition states) are appropriately symmetrized with respect to the number of identical configurations of the reactants and/or transition state. Where possible, tunneling and quantum reflection have been considered by using the corresponding imaginary frequency of the transition state and calculating the tunneling probability for the corresponding Eckart barrier. After all microcanonical rate constants have been calculated, the master equation is solved for the particular energy in order to take account of the possibility of interconversion between intermediates. We set up a matrix k of the rate constants such that the off-diagonal element k_{ij} represents the rate constant from species j to species i and the diagonal elements are such that the sum of each column is 0. Moreover, we set up a concentration vector c such that the element c_j corresponds to the concentration of channel j. Then, all kinetics expressions can be written as a vector differential equation

$$\frac{dc}{dt}=k*c.$$

This is a linear differential equation and thus can be solved using standard methods. In order to determine the behavior of c in the infinite future we diagonalize the matrix k and determine its eigenvectors. These eigenvectors will either correspond to eigenvalues with a negative real part (vanishing in the infinite future) or 0 (stable eigenvectors). The initial concentration vector (as determined by capture theory among the three possible initial intermediate) is written as a linear combination of all eigenvectors and, subsequently, those with a negative eigenvalue are discarded. What remains is the concentration vector in the infinite future, yielding the branching ratios of all channels.

3. RESULTS AND DISCUSSION

3.1. Electronic Structure Calculations

Starting from the results obtained by Basiuk & Bogillo (2002), the structures of all the stationary points were re-analyzed at higher levels of theory, i.e., B2PLYP-D3/m-aug-cc-pVTZ geometry optimizations with subsequent energy determinations also at the CBS-QB3 level. The reliability of the B2PLYP computational model is confirmed by the close correspondence of relative energies with their CBS-QB3 counterparts (cf. Figure 1 and Appendix). All the precursors, intermediates, and products were fully characterized as minima on the potential energy surface and transition states exhibited a single imaginary frequency.

Figure 1 depicts possible reaction paths of the full $^{\cdot}$CN + CH_2NH $\rightarrow$ E-C-, Z-C- and N-cyanomethanimine formation reactions. Two pathways have been considered for each case, the first in one step (red) with one transition state (2Z, 2E and $2N_\beta$), and the second (blue), which includes two intermediates (1 and 3) and two transition states (2C, $2N_\alpha$ and 4). Let us focus first on the pathway leading to the C-cyanomethanimines (E- and Z-). As one can see, the first step consists in $^{\cdot}$CN attacking the carbon atom of CH_2NH, leading to the (NC) $CH_2N{\cdot}H$ radical 1C, which is about 50 kcal/mol more stable. At this point, three possibilities can be envisaged. On the one hand, one might observe a loss of hydrogen radical, leading directly to the E or Z isomer, depending on the original conformation of 1C. This step has an exit barrier of about 37 kcal/mol. On the other hand, a migration of the CN moiety to the N atom can be realized through transition state 5 with a barrier of 25 kcal/mol. To finish, considering the presence of the stabilizing C$\equiv$N moiety on the carbon atom, hydrogen migration can also be observed in order to get the free electron on this atom. This migration would occur through the transition state 2C which has a barrier of ca. 32 kcal/mol, and would lead to the most stable compound involved in this reaction: the second intermediate 3C. Basiuk & Bogillo (2002) only studied this reaction up to this compound, which is a reactive radical. Therefore, they left room for continuing their study and suggested a deeper analysis including combination with several other radicals. However, they never mentioned the possible loss of a hydrogen radical, which we focus on here. This last step was found to be possible through another transition state with a significant barrier of about 56 kcal/mol, and leads either to E-C-cyanomethanimine or its Z isomer and a $^{\cdot}$H radical. In the first case, the compounds are more stable than the reagents by 14.5 kcal/mol and in the second case by 15.4 kcal/mol. When concentrating on the pathway to N-cyanomethanimine, one can notice a similarity with the previous route. In that case, the $^{\cdot}$CN attack occurs toward the nitrogen atom, leading to a first intermediate 1N that is slightly more stable than the other path's (1C—of about 2 kcal/mol). From here, three

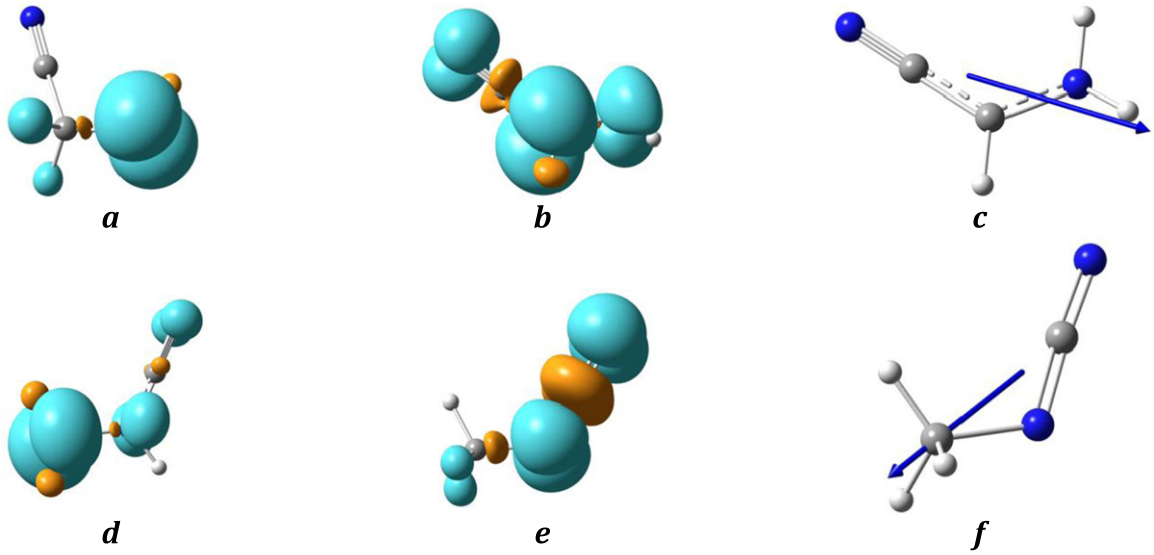

Figure 2. Spin densities of the intermediates 1C(a), 3C(b), 1N(d), and 3N(e) and dipole moments of 3C(c) and 3N(f).

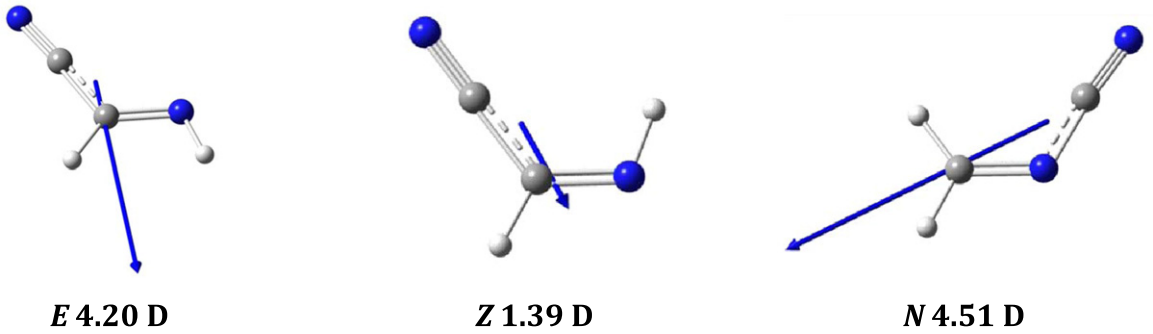

Figure 3. Dipole moments of *E*-C-, *Z*-C-, and N-cyanomethanimine.

possibilities are again envisaged: a C≡N migration to the C atom that would have a 27 kcal/mol barrier; a direct loss of hydrogen through intermediate $2N_\beta$, which would cost 47 kcal/mol; and the presence of the stabilizing C≡N moiety on the nitrogen atom that would lead to a hydrogen migration, 43 kcal/mol. This second step, which needs to go through a first transition state $2N_\alpha$, requires more energy than its counterpart on the other path: 43 versus 32 kcal/mol. Moreover, the second intermediate 3N is less stabilized than its counterpart 3C due to a shorter delocalization chain. As far as the last step is concerned, one can notice the smaller barrier (48 versus 56 kcal/mol) that leads to a less stable final compound, i.e., N-cyanomethanimine (9 versus 14.5 and 15.5 kcal/mol). These reaction paths are all feasible in the ISM considering that all the steps can be done without exceeding the allowed energy given by the two precursors. Indeed, we found possible ways to form cyanomethanimine isomers in space. The possible radical mechanisms based on the reaction paths we proposed are given in the Appendix (Figures 5–6). Another reaction path, given in the Appendix (Figure 7), focuses on an attack of the ˙NC radical leading to iso-cyanomethanimines. In Figure 2, one can see the main localization of the spin densities and dipole moments of several compounds. On the first intermediate 1, a major contribution can be seen on the atom not linked to C≡N, ensuring the presence of the free electron on this atom. In the case of compound 3C, one can observe the more delocalized spin density, which is linked to the delocalized free electron. The contribution of the carbon is the most important, however. This phenomenon is also noticeable on 3N, but constrained to the N-C≡N moiety. The dipole moments of 3C and 3N, as far as they are concerned, start from the averages of both conjugation chains.

After verifying that the formation of the three isomers is feasible in the ISM because of the lack of entrance channels, we consider here the further dissociation that *Z* and *N* could undergo because they are formed by very exothermic processes and are, therefore, characterized by a non-negligible excess of internal energy. In Figures 11 and 12, one can see that these reactions would require too much energy to occur in the ISM. A cyclization has also been envisaged, but the resulting cycle (azirin-2-imine) would also be too energetic. Let us now focus on the detection of the three isomers by microwave (MW) spectroscopy. As mentioned before, line intensities strongly depend on the dipole moments of the compounds of interest. Figure 3 depicts the dipole moment orientations and values of *E*-C, *Z*-C-, and N-cyanomethanimine. One can see that the *Z* isomer has a very small dipole moment compared to *E* and *N*, which could explain why it is difficult to detect by MW in space. Also N-cyanomethanimine has not yet been characterized conclusively in space, although several rotational transitions that could correspond to this compound have been observed by Zaleski et al. (2013). In any case this compound is not thermodynamically favored compared to its C-isomers (less

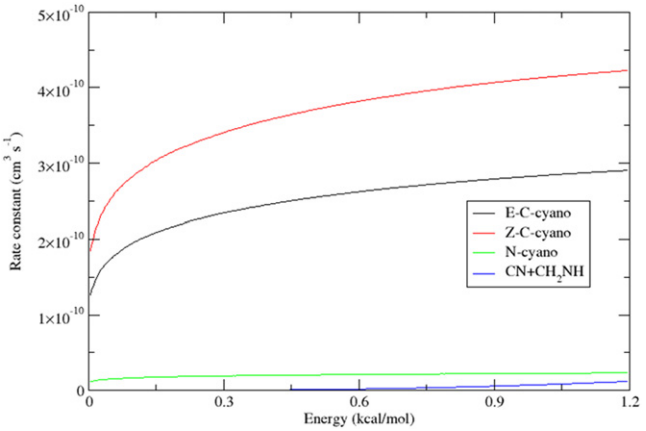

Figure 4. Rate constants of final products.

stable by 6 kcal/mol), which would also explain a reduced presence in the ISM.

3.2. Kinetics Calculations

We have performed calculations for total energies (taking as zero the zero-point energy of the reactants CN + CH_2NH) of up to 1.2 kcal/mol. As the most probable collision energy at 100 K is 0.2 kcal/mol, we believe that this range of energies adequately describes the reaction scheme at the temperatures of the ISM.

As an initial step, we have calculated the capture rate constant for the initial CN + CH_2NH reaction. In order to do this, we performed calculations for various points along the entrance coordinate CN-CH_2NH and we subsequently fitted the energies to a $V = V_0 - \frac{C_6}{R^6}$ law to determine the C_6 constant which was used in the capture theory calculation. There are three possible initial adducts. Two of them are cyano adducts (i.e., CN adds through its C atom, either on the C or the N atom of the methanimine) and one is an isocyano adduct (CN adds through its N atom on the C atom of the methanimine). We have partitioned the initial overall capture rate constant among the three adducts in proportion to their densities of states at the energy considered. It must be stressed that it is the translational (collision) rather than the total energy that appears in the capture rate expression.

The final product specific rate constants appear in Figure 4 for all energies considered. At all energies, the rate constant for the production of iso-cyano products was found to be negligible. This fact is easy to understand since, as can be seen from the energy table, the energies for all transition states from the initial iso-cyano adduct are well above the reactants and hence the only contribution from these is due to tunnelling. Moreover, the density of states of the initial iso-cyano adduct is about two orders of magnitude lower than the others. Regarding the products observed, it is seen that the rate constant is maximum for the *Z*-C-cyano product with the *E*-C-cyano product following (the respective branching ratios are around 57% and 39%).

The reason for the prevalence of the *Z* product is the slightly lower energy of the respective transition states compared to the *E* ones. On the other hand, the branching ratio of the N-cyano product is only around 4%. This is in spite of the fact that the density of states of the initial N-adduct is higher than that of the initial C-adduct and thus its initial population is higher. As can be seen, the barriers for hydrogen migration and elimination from the N-adduct are much higher than those for the C-adduct and, moreover, the barrier for interconversion between C- and N-adduct is considerably lower.

As a result, the initial populations do not play much of a role. It is rather the subsequent barriers that determine the final outcome. Finally, back-dissociation into reactants is negligibly slow at low energies, whereas it reaches a branching ratio of around 1% to 1.5% at the highest energy. It can be seen from Figure 5 that the rate constant rises rather steeply towards the high energy end—the reason for this being the high density of states of the reactants (which comprises five rotational degrees of freedom).

The rate constants as functions of temperature have been obtained through Boltzmann weighting of the microcanonical values and subsequently fitted (for each product) to the expression:

$$k(T) = \alpha * (T/300\ \mathrm{K})^{\beta} * e^{-\frac{\gamma}{T}}.$$

In Table 1, the three parameters corresponding to each of the three products are shown. Among the three parameters, γ represents the activation energy at 0 K. In all cases this is positive, both as a result of the capture rate constant (it is increasing as a function of energy) and the subsequent energy barriers for the unimolecular steps. The exponent β is the first derivative of the activation energy with temperature (its dependence on temperature is assumed to be linear in this model) and represents the entropy effect on the activation energy. It is positive in all cases, reflecting an increase of the activation energy with temperature and a negative activation entropy.

4. CONCLUSION

In this paper, we have provided new insights into the formation of cyanomethanimine isomers in the ISM. Our electronic structure and kinetic calculations demonstrate that the reaction CN + CH_2 = NH is a facile formation route of *Z*,*E*-C-cyanomethanimine, even under the extreme conditions of density and temperature typical of cold interstellar clouds. The rate coefficients for *Z*-C-cyanomethanimine and *E*-C-cyanomethanimine formation are 2.7×10^{-10} and 1.8×10^{-10} $cm^3\ s^{-1}$, respectively, at the temperature of 10 K (and 3.8×10^{-10} and 2.6×10^{-10} $cm^3\ s^{-1}$, respectively, at 100 K), that is, they approach the gas kinetic limit. Therefore, in all cases where the CN radical and methanimine are relatively abundant, we can expect to observe some cyanomethanimine as well. We also note that, since the formation of the more stable *Z*-isomer is favored by a factor of ca. 1.5 and since the detection of the *E*-isomer is favored by a factor of 6 (Zaleski et al. 2013), the missing detection of the *Z*-isomer can be due to the sensitivity limit of the GBT PRIMOS survey, as already suggested by Zaleski et al. (2013). The detection of the *Z*-isomer should be attempted with more sensitive instrumentation to verify the proposed formation mechanism of C-cyanomethanimine isomers. N-cyanomethanimine is formed with a much lower probability and its detection will be extremely challenging. We recall that cyanomethanimine is an important species in the context of prebiotic chemistry, essentially because of its role as an intermediate in adenine formation (Oro 1961; Evans et al. 1991; Matthews 1995; Eschenmoser 2007; Balucani 2012; Jung & Choe 2013). Since the dimerization of HCN to cyanomethanimine was already proven to be a difficult step in the absence of liquid water (Smith et al. 2001; Yim & Choe 2012), the reaction investigated here can be regarded as a

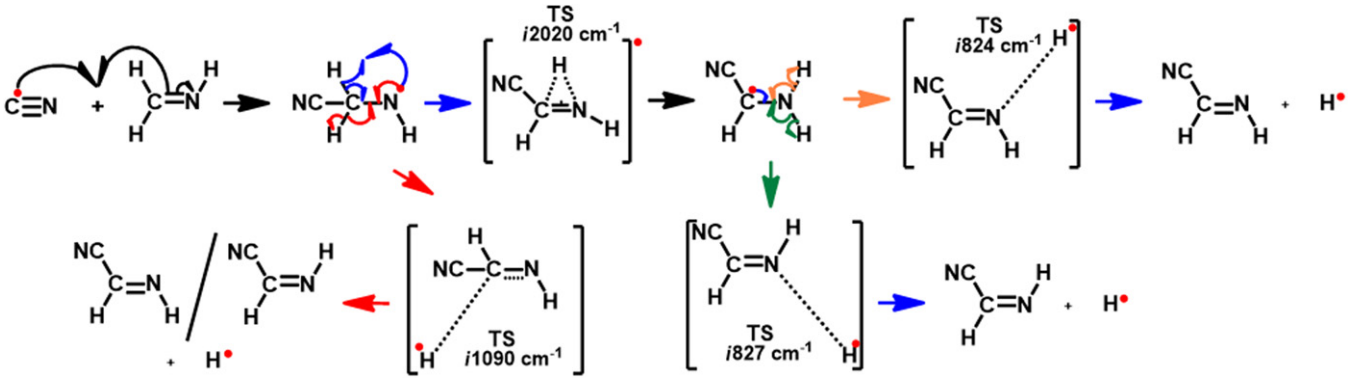

Figure 5. Possible formation mechanisms of *E*- and *Z*-C-cyanomethanimines.

Table 1
Parameters of the Fitting with Respect to the Product

	α (cm^3 s^{-1})	β	γ (K)
E	3.15×10^{-10}	0.152	9.05×10^{-02}
Z	4.59×10^{-10}	0.153	8.71×10^{-02}
N	2.44×10^{-11}	0.121	0.115

potential shortcut toward the formation of adenine in extra-terrestrial environments that allows the bottleneck of HCN dimerization to be avoided (Roy et al. 2007; Andersen et al. 2013). Finally, since both CN radicals and methanimine are important species in the upper atmosphere of Titan (with methanimine being formed by the reaction N(^{2}D) + CH_4 and C_2H_6; see Balucani et al. 2009, 2010 and Loison et al. 2015), we suggest that the CN +CH_2NH reaction could significantly contribute to the build up of the nitrogen-rich organic aerosols (Israel et al. 2005) that cover the massive moon of Saturn.

A more general conclusion is that neutral–neutral gas-phase reactions can account for the formation of relatively complex organic molecules (COM) even under the extreme conditions of the ISM. Ice-catalyzed reactions are often called into play to explain the formation of COMs because of supposedly missing formation routes in the gas phase, but not all possible gas-phase routes have been actually explored, either in laboratory experiments or theoretically (Balucani et al. 2015a). Other studies of critical and yet unexplored neutral–neutral gas phase reactions performed with the same theoretical methods employed here can help to fulfill the gap of the missing reactions leading to COMs, especially when those reactions cannot be easily investigated in laboratory experiments as in the present case.

The research leading to these results has received funding from the European Union's Seventh Framework Programme (FP7/2007-2013) under grant agreement No. ERC-2012-AdG-320951-DREAMS.

APPENDIX

This appendix presents the optimized parameters of all stationary points compound + electronic energies, imaginary frequencies for transition states, comparison between computed energies via CBS-QB3 and B2PLYP-D3/m-aug-cc-pVTZ, possible reaction paths (Figures 6 and 7), information on resonance forms (Figure 8) and delocalization chains (Figure 9), and the envisaged dissociations of *Z* and N compounds (Figures 10–12). A table including some selected bond lengths is also given (Table 2).

Optimized Parameters—Electronic Energies at the CBS Level of Theory

Precursor CN E_{el} = −92.592407 AU			
Atom	*X*	*Y*	*Z*
C	−0.6319015859526	0.0000000000000	0.0000000000000
N	0.5415110301566	0.0000000000000	0.0000000000000
Precursor CH_2NH E_{el} = −94.504654 AU			
Atom	*X*	*Y*	*Z*
C	−0.6296222769770	−0.0184458250452	0.0000000000000
H	−1.2265531985047	0.8893031075475	0.0000000000000
H	−1.1770138983161	−0.9623152679322	0.0000000000000
N	0.6354594064232	0.0815530698565	0.0000000000000
H	1.0710761145589	−0.8404834747094	0.0000000000000
1C E_{el} = −187.173406 AU			
Atom	*X*	*Y*	*Z*
C	0.6643573263464	0.5893575599881	−0.0087509264592
H	0.8322504675228	1.2675229637755	0.8304958508515
H	0.8340495445553	1.1929333557147	−0.9086728441313
N	1.6698967675533	−0.4469820075484	0.0216317281397
H	1.2240864161769	−1.3430020576361	−0.1860797707662
C	−0.7321723715889	0.1390780570606	−0.0011312499816
N	−1.8198083701693	−0.2576793962081	0.0058558578055
2C E_{el} = −187.121703 AU			
Atom	*X*	*Y*	*Z*
C	−0.6101807072605	0.5505966471317	−0.0112670952585
H	−1.3393771024981	0.2776427698866	−0.9912074558559
H	−0.8373879100916	1.5554578737104	0.3113979689562
N	−1.7138058828331	−0.3784278062894	0.0584238661775
H	−1.3323050262241	−1.3094651333815	−0.1180249990287
C	0.7482280403580	0.1309569961062	0.0104563333508
N	1.8480593077211	−0.2433197250982	−0.0003075759452
2E E_{el} = −187.114678 AU			
Atom	*X*	*Y*	*Z*
C	−0.6820422123230	0.4405223038146	−0.1351119979507
H	−0.8507140943617	1.4142703873105	−0.5931499384699
H	−0.6125687157932	1.4127015235405	1.4253249693055
N	−1.5880049911338	−0.4444086984492	0.0639583960933
H	−2.5085436848483	−0.0521515010221	−0.1285618408562
C	0.7164728060308	0.0660530868994	−0.0245402983044
N	1.8443586358935	−0.1894120016129	0.0222161513773

(Continued)

2Z E_{el} = −187.115738 AU			
Atom	X	Y	Z
C	−0.6896677262448	0.4567559294068	−0.1208862986250
H	−0.8972406468772	1.4374221967930	−0.5361331891121
H	−0.6314738103893	1.3720099344771	1.4784648306040
N	−1.6526129508561	−0.3782283703200	0.0169819058829
H	−1.3117354216988	−1.2892859870369	0.3228281405311
C	0.7180526364032	0.1015137902544	−0.0291164341546
N	1.8327203744849	−0.2095909881500	0.0205079401985

3C E_{el} = −187.207783 AU			
Atom	X	Y	Z
C	0.5910997532836	0.5470182149226	−0.0150499225437
H	0.8310506421540	1.5945985251626	0.0294757650816
N	1.6234959781206	−0.3595805752933	0.0421543452085
H	1.4201181898135	−1.3171015055985	−0.1904994296445
C	−0.7347391191169	0.1269223903726	−0.0001327763747
N	−1.8448167447930	−0.2349391550464	−0.0002961206979
H	2.5342287203474	−0.0415269742786	−0.2397913715940

4E E_{el} = −187.117724 AU			
Atom	X	Y	Z
C	−0.6348927273746	0.5178489236241	0.0801768470045
H	−0.7784266820035	1.5617776548760	0.3497440948007
N	−1.5762380094672	−0.3098368725442	−0.1455098961346
H	−1.8689650105727	−1.7302901552569	1.0054967044100
C	0.7375762642202	0.0865320719247	0.0089907355460
N	1.8577718992931	−0.2057480630933	−0.0246979347943
H	−2.4869740427134	0.1359692173294	−0.0520167132706

4Z E_{el}=−1.7.118568 AU			
Atom	X	Y	Z
C	−0.6330918888058	0.5095011569744	−0.0144075405497
H	−0.8295535016531	1.5726688412691	0.0653255147371
N	−1.6111744501605	−0.3002849350155	−0.1117335270135
H	−1.3046057552862	−1.2704949142092	−0.1752551475842
C	0.7529093663965	0.1114770926446	0.0147556511599
N	1.8641833167440	−0.2176405453273	0.0267970862032
H	−2.8078807119858	−0.4998175221737	1.2859213931323

1N E_{el} = −1.7.128363 AU			
Atom	X	Y	Z
C	−1.6642966005388	−0.4073823836941	0.0321345156571
H	−1.4434627298269	−1.4459060140602	−0.1279806973969
H	−2.6459915648770	0.0047162359001	−0.1073577838209
N	−0.5979859026835	0.4877610400582	−0.0184745554441
H	−0.7799642456439	1.4731145429049	0.0723625050339
C	0.6798611355568	0.1084604417483	−0.0003428583623
N	1.7920628239957	−0.2338961583824	0.0029602035107

2N$_\alpha$ E_{el} = −187.064315 AU			
Atom	X	Y	Z
C	1.6341536771190	−0.4105303766349	−0.0055719949309
H	1.3964810358640	−1.4599608504861	0.0840701844438
H	2.6056574098826	−0.0273644784208	0.2570755205135
N	0.5823854114773	0.5799720098118	0.0508035544699
H	1.1733391618214	0.3352770518764	−0.9901044227493
C	−0.6688748246221	0.1067594986372	0.0066834020785
N	−1.7820735750695	−0.2367392574425	−0.0050493181049

2Nβ E_{el}=−187.061811 AU			
Atom	X	Y	Z
C	1.5773528712952	−0.4040447530435	0.0397076553162
H	1.3860486141028	−1.4332509051199	0.3239772076390
H	2.5976711103342	−0.0695667090500	−0.0873933070444
N	0.6412534209867	0.4637571884582	−0.1186373470059
H	0.6725256869684	1.8716030633730	0.7928564996342
C	−0.6438265369723	0.0600428558145	−0.0136704431435
N	−1.7763610914043	−0.1955052635156	0.0222340605025

3N E_{el} = −187.137477 AU			
Atom	X	Y	Z
N	0.5290824088209	−0.5746498315317	−0.0000017726213
C	−0.6631140903156	−0.1042726587737	0.0000009974756
N	−1.7946797921902	0.2414729086697	−0.0000001669476
C	1.6468718572164	0.3527750001544	−0.0000024389613
H	2.2589437455342	0.1352024110059	0.8753175016506
H	2.2592080764213	0.1348984715159	−0.8750567747740
H	1.3530662998495	1.4003011716258	−0.0002166143050

4N E_{el} = −187.070416 AU			
Atom	X	Y	Z
N	−0.5955416608502	−0.5354514908029	0.0741559974496
C	0.6655928389347	−0.0849894453480	0.0109638603989
N	1.7913350184451	0.2060873789852	−0.0138484093390
C	−1.5587973195680	0.2775133315528	−0.1621110932045
H	−1.4089329609028	1.3031429627358	−0.4917545926481
H	−2.5659258859820	−0.1184112393929	−0.1488315258078
H	−2.0046801562490	1.0992196713932	1.6023355675426

E-C-cyanomethanimine E_{el} = −186.620334 AU			
Atom	X	Y	Z
C	0.6872192345753	−0.4730489077173	−0.0000000551828
H	0.8521205045785	−1.5495658042040	0.0000008752927
N	1.6017184239642	0.4094023739145	−0.0000000867090
C	−0.7013479833823	−0.0767499544759	−0.0000006500446
N	−1.8322541025699	0.1757509235582	0.0000004263429
H	2.5192515391225	−0.0343982030495	0.0000028027356

Z-C-cyanomethanimine E_{el} = −186.621633 AU			
Atom	X	Y	Z
C	0.6948441746923	−0.4872308656171	0.0000000000000
H	0.8989366336250	−1.5527850607095	0.0000000000000
N	1.6648550352349	0.3347450472895	0.0000000000000
C	−0.7020143510890	−0.1126712032417	0.0000000000000
N	−1.8194597861106	0.1975233583502	0.0000000000000
H	1.3345699797485	1.3001925564152	0.0000000000000

N-cyanomethanimine E_{el} = −186.611271 AU			
Atom	X	Y	Z
C	−1.5929059921035	−0.3437080587715	0.0000000000000
H	−2.6086132431199	0.0304071240223	0.0000000000000
H	−1.4324205161642	−1.4195313616157	0.0000000000000
N	−0.6440082503428	0.5102533230010	0.0000000000000
C	0.6281379460624	0.0796114714881	0.0000000000000
N	1.7616108240006	−0.1839568804526	0.0000000000000

Imaginary Frequencies for Transition States
2C 2020 cm^{-1}
2E1093 cm^{-1}
2Z1088 cm^{-1}
2N 2012 cm^{-1}
4E824 cm^{-1}
4Z_α 827 cm^{-1}
4Z_β 1327 cm^{-1}
4N 637 cm^{-1}

Computed Energies via B2PLYP-D3/m-aug-cc-pVTZ vs. CBS-QB3 Level of Theory

		E-C-cyano				
		B2PLYP-D3/m-aug		CBS-QB		
		E (kcal/mol)	Rel. *E*	*E* (AU)	*E* (kcal/mol)	Rel. *E*
ZPE-corrected energy	$CN+CH_2NH$	−117949.89	0.00	−187.05	−117843.27	0.00
	1C	−117999.92	−50.04	−187.13	−117889.35	−46.09
	2C	−117968.00	−18.11	−187.08	−117858.61	−15.34
	3C	−118019.56	−69.67	−187.16	−117909.80	−66.54
	4*E*	−117967.64	−17.75	−187.08	−117859.07	−15.80
	E-cyano +H	−117970.81	−20.92	−187.08	−117861.10	−17.84

		Z-C-cyano				
		B2PLYP-D3/m-aug		CBS-QB		
		E (kcal/mol)	Rel. *E*	*E* (AU)	*E* (kcal/mol)	Rel. *E*
ZPE-corrected energy	$CN+CH_2NH$	−117949.89	0.00	−187.05	−117843.27	0.00
	1C	−117999.92	−50.04	−187.13	−117889.35	−46.09
	2C	−117968.00	−18.11	−187.08	−117858.61	−15.34
	3C	−118019.56	−69.67	−187.16	−117909.80	−66.54
	4Z	−117968.14	−18.26	−187.08	−117859.57	−16.30
	Z-cyano + H	−117971.34	−21.46	−187.08	−117861.85	−18.59

		N-cyano				
		B2PLYP-D3/m-aug		CBS-QB		
		E (kcal/mol)	Rel. *E*	*E* (AU)	*E* (kcal/mol)	Rel. *E*
ZPE-corrected energy	$CN+CH_2NH$	−117949.89	0.00	−187.05	−117843.27	0.00
	1N	−118002.17	−52.29	−187.13	−117890.87	−47.60
	2N	−117960.48	−10.59	−187.06	−117850.52	−7.25
	3N	−118005.72	−55.84	−187.14	−117896.61	−53.34
	4N	−117962.81	−12.92	−187.07	−117854.36	−11.10
	N-cyano + H	−117965.63	−15.74	−187.07	−117855.73	−12.47

Table 2
Selected Bond Lengths (Å) of the Investigated Compounds

	Precursors		1		2					3		4			Products		
	CN	CH_2NH	C	N	C	N_α	*E*	*Z*	N_β	C	N	*E*	*Z*	N	*E*	*Z*	N
1-2	⋯	1.27	1.44	1.39	1.44	1.44	1.28	1.28	1.29	1.38	1.45	1.27	1.27	1.28	1.27	1.27	1.28
1-3	⋯	⋯	1.47	1.33	1.42	1.34	1.45	1.45	1.35	1.39	1.28	1.44	1.44	1.34	1.44	1.45	1.34
3-4	1.17	⋯	1.16	1.16	1.16	1.17	1.16	1.16	1.16	1.17	1.18	1.16	1.16	1.16	1.16	1.16	1.16
2-5	⋯	⋯	⋯	⋯	1.29	1.32	1.84	1.84	1.68	⋯	⋯	1.85	1.85	2.00	⋯	⋯	⋯

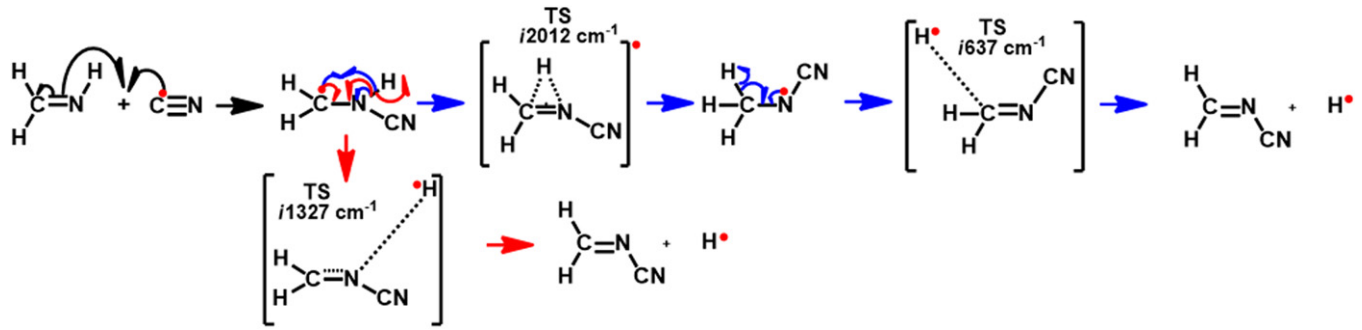

Figure 6. Possible formation mechanisms of N-cyanomethanimine.

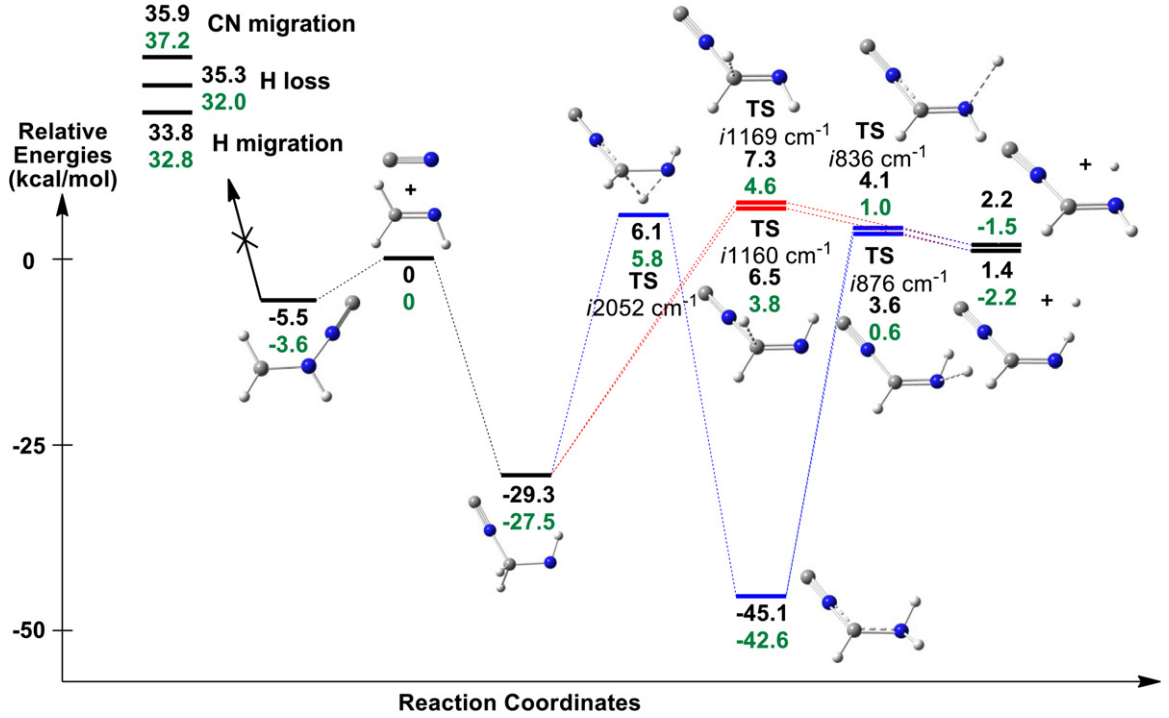

Figure 7. Reaction path leading to *E*-C- and *Z*-C-isocyanomethanimine with relative electronic energies (black) and zero-point corrected energy (green). The energies were computed using the CBS-QB3 level of theory. Alternative pathways in blue and red.

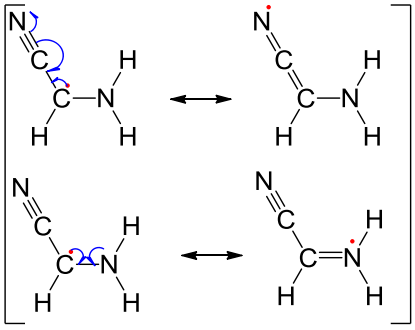

Figure 8. Resonant forms of compound 3C.

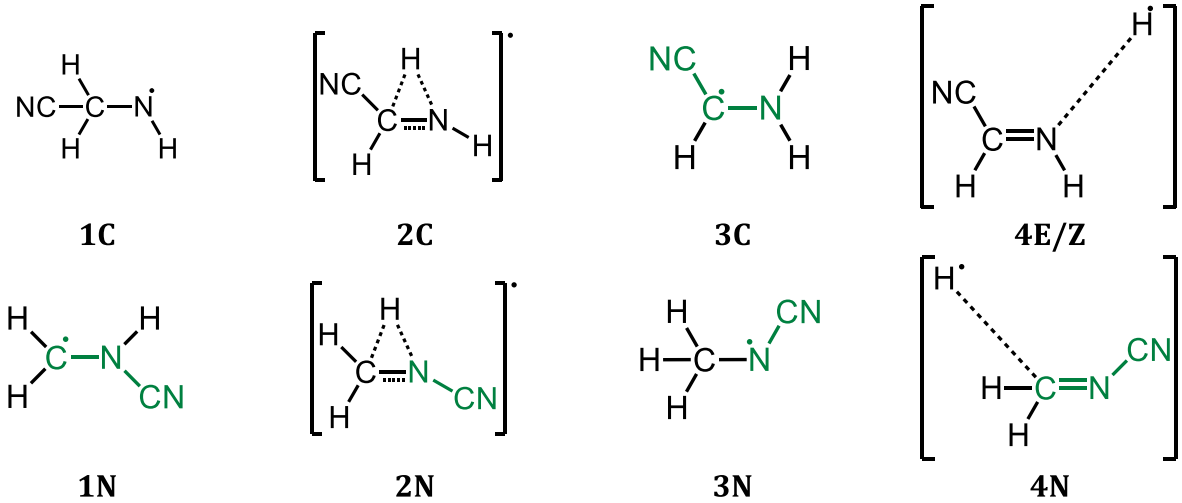

Figure 9. Delocalization chains of intermediates and transition states (green).

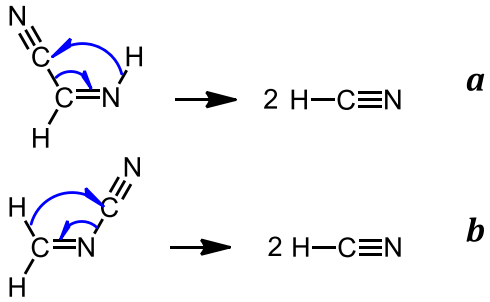

Figure 10. Envisaged mechanisms for *Z*-C- (a) and N-cyanomethanimine (b) dissociations.

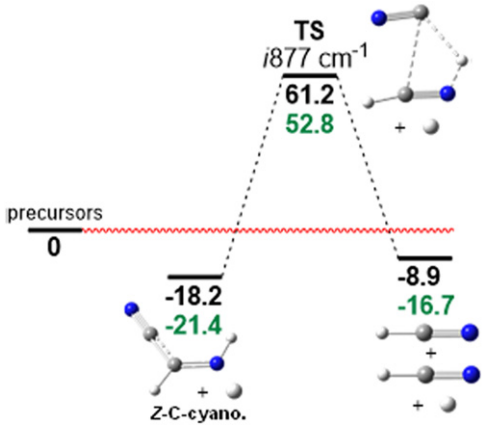

Figure 11. Reaction path for *Z*-C-cyanomethanimine dissociation (relative electronic energy (black) and zero-point corrected energy (green) in kcal/mol). Theory level: B2PLYP-D3/m-aug-cc-pVTZ.

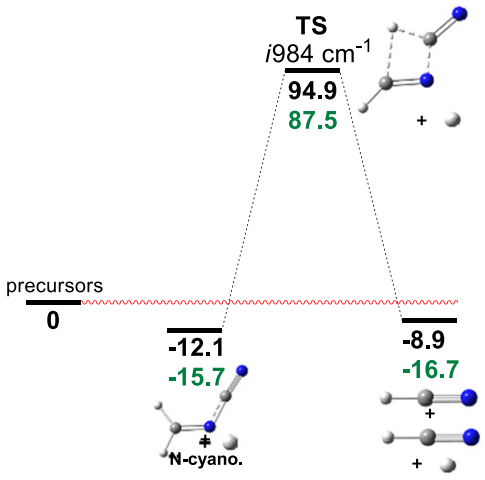

Figure 12. Reaction path for N-cyanomethanimine dissociation (relative electronic energy (black) and zero-point corrected energy (green) in kcal/mol). Theory level: B2PLYP-D3/m-aug-cc-pVTZ.

REFERENCES

Andersen, J. L., Andersen, T., Flamm, C., et al. 2013, Entrp, 15, 4066
Balucani, N. 2012, Chem Soc Rev, 41, 5473
Balucani, N., Bergeat, A., Cartechini, L., et al. 2009, JPCA, 113, 11138
Balucani, N., Ceccarelli, C., & Taquet, V. 2015a, MNRAS, 449, L16
Balucani, N., Leonori, F., Petrucci, R., et al. 2015b, CP, 449, 34
Balucani, N., Leonori, F., Petrucci, R., et al. 2010, FaDi, 147, 189
Basiuk, V. A., & Bogillo, V. I. 2002, AdSpR, 30, 1445
Biczysko, M., Panek, A., Scalmani, G., & Barone, V. 2010, JCTC, 6, 2115
Chakrabarti, S., & Chakrabarti, S. K. 2000, AA, 354, L6
Dunning, T. H. 1989, JChPh, 90, 1007
Eschenmoser, A. 2007, Tetrahedron, 63, 12821
Evans, R. A., Lorencak, O., Ha, T.-K., & Wentrup, C. 1991, JAChS, 113, 7261
Frisch, M. J., Trucks, G. W., Schlegel, H. B., et al. 2014, Gaussian GDVH37p
Goerigk, L., & Grimme, S. 2011, JCTC, 7, 291
Grimme, S. 2006, JChPh, 124, 034108
Grimme, S., Antony, J., Ehrlich, S., et al. 2010, JChPh, 132, 154104
Israel, G., Szopa, C., Raulin, F., et al. 2005, Natur, 438, 796
Jung, S. H., & Choe, J. C. 2013, AsBio, 13, 465
Leonori, F., Petrucci, R., Balucani, N., et al. 2009, JPCA, 113, 15328
Leonori, F., Skouteris, D., Petrucci, R., et al. 2013, JChPh, 138, 024311
Loison, J. C., Hebrard, E., Dobrijevic, M., et al. 2015, Icar, 247, 218
Matthews, C. N. 1995, PSS, 43, 1365
McElroy, D., Walsh, C., Markwick, A. J., et al. 2013, AA, 550, A36
Montgomery, J. A., Frisch, M. J., Ochterski, J. W., et al. 2000, JChPh, 112, 6532
Ochterski, J. W., Petersson, G. A., & Montgomery, J. A. 1996, JChPh, 104, 2598
Oro, J. 1961, Natur, 191, 1193
Papajak, E., Leverentz, H. R., Zheng, J., et al. 2009, JCTC, 5, 1197
Puzzarini, C., Ali, A., Biczysko, M., et al. 2014a, ApJ, 792, 118
Puzzarini, C., Biczysko, M., Bloino, J., et al. 2014b, ApJ, 785, 107
Roy, D., Najafian, K., & von Ragué Schleyer, P. 2007, PNAS, 104, 17272
Smith, I. W. M., Talbi, D., & Herbst, E. 2001, AA, 369, 611
Vazart, F., Calderini, D., Skouteris, D., et al. 2015, JCTC, 11, 1165
Wakelam, V., Herbst, E., Loiso, J.-C., et al. 2012, ApJS, 199, 21
Yim, M., & Choe, J. 2012, CPL, 538, 24
Zaleski, D. P., Seifert, N. A., Steber, A. L., et al. 2013, ApJ, 765, L10